Semiconductor Physics, Quantum Electronics & Optoelectronics, 2025. V. 28, No 3. P. 374-382.

Sensors

Optimization of chromatic SPR sensor of gas environment based on registration of reflected beam color: Modeling and experiment

O.L. Kukla, Yu.M. Shirshov, A.I. Biletskiy, O.M. Fedchenko, O.S. Kondratenko

V. Lashkaryov Institute of Semiconductor Physics, National Academy of Sciences of Ukraine,
41 Nauky Avenue, 03028 Kyiv, Ukraine
**Corresponding author e-mail: alex.le.kukla@gmail.com*

Abstract. Optical characteristics of a chromatic sensor for detecting gas media based on the surface plasmon-polariton resonance (SPR) effect were calculated during recording color spectrum responses of the reflected beam. At this, spectral characteristics of all the components of the optical system (radiation source, photodetectors and multilayer reflective structure) in the visible light range were taken into account. Based on these calculations, a method for assessing the hardware sensitivity of the SPR sensor to changes in the external environment characteristics (refractive index or permittivity) was proposed. A thin silver film on the base face of a prism in the Kretschmann geometry was used as a sensitive element for modeling and experimental investigations. This enabled a full-fledged SPR effect in the entire visible spectral range of 400…700 nm. Colorimetric registration of the reflection spectra using a color webcam with R, G, B output signals as the optical response was implemented.

Keywords: spectral SPR, chromatic mode, silver film, optical gas sensor, colorimetric registration, reflected beam spectrum, R, G, B components, visible light range.

https://doi.org/10.15407/spqeo28.03.374
PACS 07.07.Df, 42.79.Pw, 42.79.Qx, 73.20.Mf, 78.40.-q, 87.85.fk

Manuscript received 01.05.25; revised version received 27.08.25; accepted for publication 03.09.25; published online 24.09.25.

1. Introduction

The surface plasmon resonance (SPR) effect [1] is the physical basis of a wide class of sensors for recording biomolecular interactions in solutions and volatile molecules in gas phase. It has been paid close attention over the past decade [2–8]. To measure sensor responses, plasmon resonance and its change under the influence of the analyzed medium are detected in several ways such as by the angle of minimum reflection or change in the reflection amplitude under monochromatic illumination, and wavelength value for a fixed angle under white light illumination [3, 4]. In the latter case, an SPR sensor operates in the spectral (chromatic) mode. It has been shown in particular that such a polychromatic recording method has undoubted advantages in the design of multichannel biosensors [1, 9, 10]. However, this requires use of expensive spectrometers in the visible and near IR region, which significantly reduces attractiveness of the method. At the same time, miniature video cameras and even smartphones have been actively used recently as optical signal recorders. A number of papers report use of a color web camera instead of a spectrophotometer to assess the change in the color of the reflected beam under white light illumination [11–22]. Application of this registration method can be expanded. For example, it is possible to register both the full multicolor reflection spectrum in a certain range of incidence angles of a diverging white light beam, or to register only a certain part of the reflection spectrum corresponding to different incidence angles. Another variant of the spectral method is to use several light sources with different wavelengths and incidence angles of a collimated beam, which alternately illuminate the sample [23]. In this case, the response is registered by measuring three color components (R, G, B) of the reflected light, or at least two of them, each being recorded at a different incidence angle.

The aim of this work is modeling of the optical characteristics of a chromatic SPR sensor for gas environments with responses recorded across the color spectrum of a reflected beam, assessing its instrumental sensitivity to changes in the external environment parameters (refractive index or permittivity), and developing approaches to creating new versions of a polychromatic SPR sensor for gas analysis based on recording the reflected beam color. A thin silver film applied to the base surface of a glass prism in the Kretschmann geometry is used as a plasmon-generating layer. This layer is capable of implementing a full-fledged SPR in the entire visible light range from

400 to 700 nm [24]. A color web camera is used to record the optical signal, followed by colorimetric analysis of the change in the color of the pattern of the reflected beam at white light illumination.

2. How the spectrum of a white beam changes after reflection in the presence of SPR

After a white light beam has penetrated the glass, it is reflected from the boundary with the silver film and exits from the opposite side of the prism. We assume that the amplitudes of the incident waves are the same in the entire visible range ($\lambda = 400…700$ nm). In the case of total internal reflection from the base face of the glass prism in contact with air, the amplitudes of the reflected waves should also be equal regardless of the wavelength. However, in the presence of a thin metal film applied to the glass, there is a dip in the reflection at certain angles of incidence due to the excitation of plasmon-polariton resonance. The depth of this dip depends on the dielectric function of the metal and the angle of light incidence. This means that some color bands will be removed from the white spectrum. As a result, the reflected beam acquires a color complementary to the color component absorbed by the metal and causing the SPR effect at a given incidence angle.

Fig. 1a shows an optical scheme in the Kretschmann geometry, which is the basis for both model calculations and real experiments using different wavelengths to excite SPR. Here, the flat front of a slightly diverging white beam is conditionally divided into several sections of a certain width ($n = 4$ in this case) following the increasing incidence angle $\theta_1...\theta_n$. The reflected colored stripes of the beams are directed to a recording device (web camera) and recorded as a set of spectral bands of different colors perpendicular to the base of the prism (Fig. 1b). It is obvious that spatial arrangement of these bands is uniquely related to the changing incidence angle.

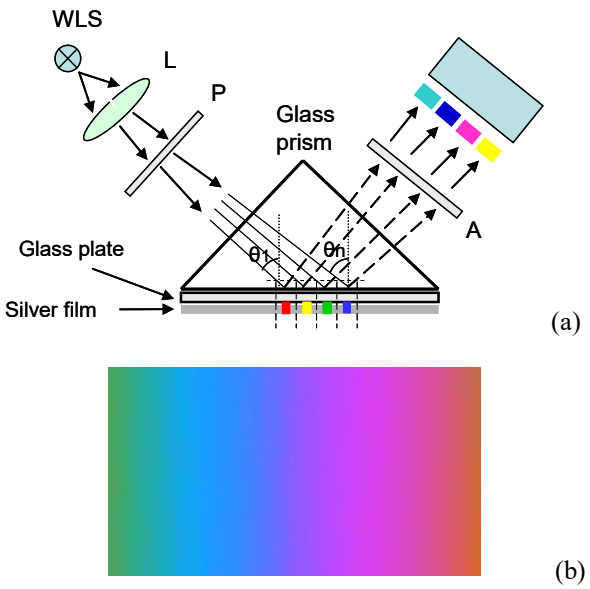

Fig. 1. (a) Optical scheme for implementation of spectral SPR in the Kretschmann geometry: WLS – white light source, L – lens, P – polarizer, A – analyzer. (b) spectrum of a reflected light recorded by a webcam.

We calculate angular dependence of the spectrum of the reflected beam upon excitation of SPR in a 40-nm thick silver film in the Kretschman geometry for a 90-degree glass prism with a refractive index of 1.51. The spectral dependences of the optical constants for silver are taken from the data given in [4]. Since the optical scheme of the sensor used in Fig. 1 includes a set of different optical units, to obtain the resulting spectral dependence, the integral transfer function of the optical system should be calculated taking into account all its components: the light source, the reflective metal film and the photodetectors of the video camera.

Fig. 2 shows the experimental emission spectra of the used light source, the photosensitivity of the webcam detectors, and the model spectral dependences of the reflection coefficient of the silver film in the visible light wavelength range of 400 to 700 nm for the incidence angles within 42…52 degrees.

The light source spectrum was measured using a Blue-Wave StellarNet spectrophotometer. The photosensitivity spectra of the webcam were studied using a DMR-4 monochromator with quartz prisms (diameter of the output aperture of 3 mm, width of the input and output slits of 0.65 mm, and spectral width of the slit of 5…10 nm). The radiation source was a halogen incandescent lamp KGM-150. A Si photodiode S1337-1010bq Hamamatsu was used as a calibration photodetector. In order to equalize the radiation intensity along the spectrum, a set of filters with a calibrated transmission level was used.

To obtain the spectral functions of the reflection coefficient $R(\lambda, \theta)$ in the given wavelength range and at the given light incidence angles, traditional formulas for reflection of light from a multilayer structure were used applying Johnson matrix multiplication [25].

The data shown in Figs. 2a–2d allow us to calculate the angular dependence of the spectrum of the reflected beam in the optical scheme shown in Fig. 1. Thereafter, the change in the color of the reflected beam when the refraction coefficient of the environment changes can be traced. This justifies use of the SPR-RGB effect for implementing a gas sensor in the spectral version.

For calculations, we use the following information. We take into account that the webcam registers radiation in a certain wavelength band for each color component, having bell-shaped and partly overlapping spectral characteristics. We assume for definiteness that the color components R, G, B of a three-color webcam correspond to the wavelengths λ_k = 600, 530 and 420 nm, where the index k refers to one of the three color components (the specified values of λ_k in this case are related to the characteristics of the color filters of the camera photosensitive matrix). Note that the white light source has a continuous, but highly uneven spectral characteristic.

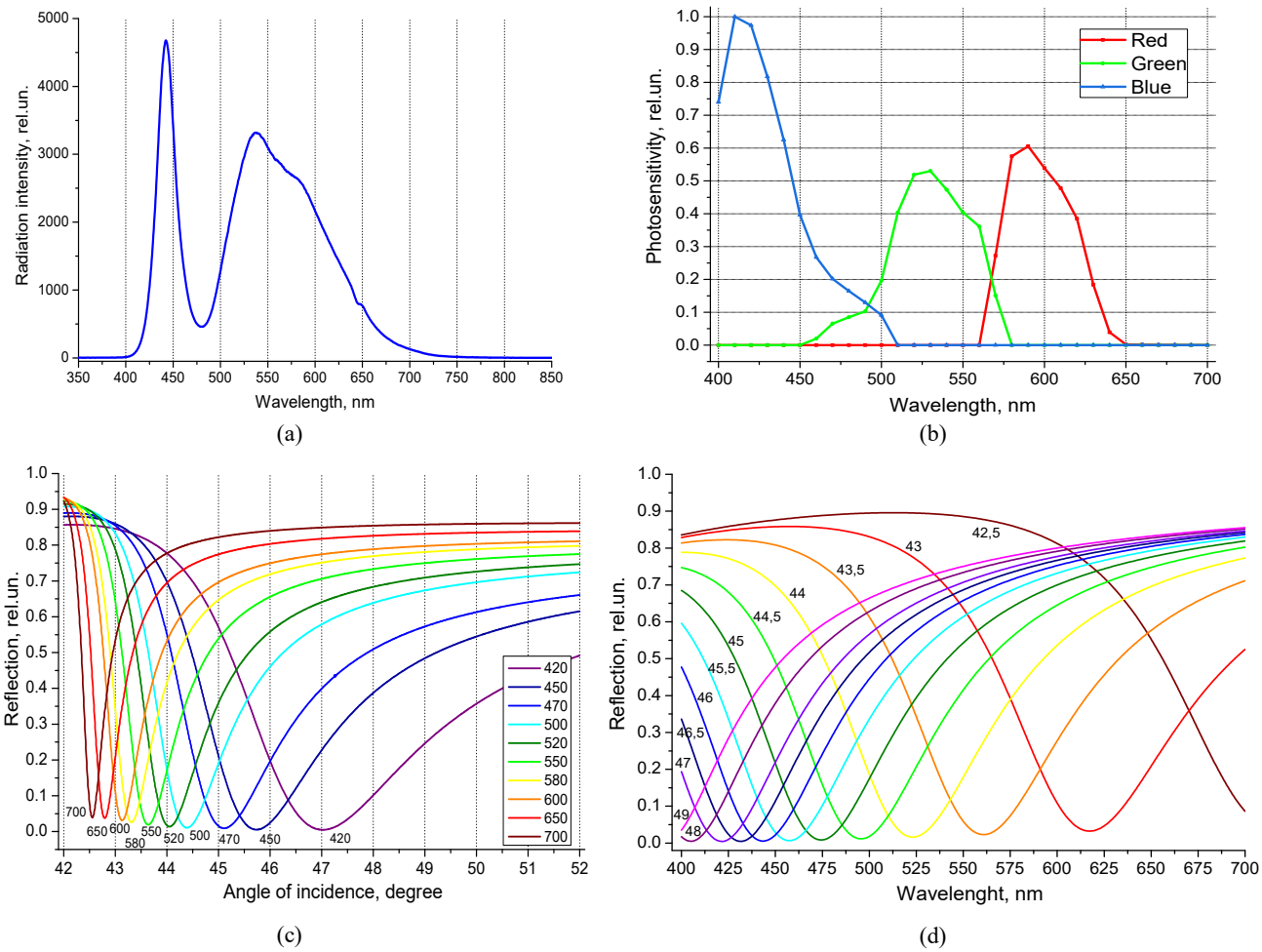

Fig. 2. (a) Emission spectrum of a super-bright LED CreeXTE Star 5W White 5000K, (b) photosensitivity spectra of the photodetector matrix of a webcam Logitech C525, (c) spectral dependences of the reflection coefficient of a 40-nm thick silver film on a glass prism K8 ($N_g = 1.515$) in contact with air ($\varepsilon_d = 1$) in the range of light incidence angles $\theta = 42\ldots52$ deg. for a number of specified wavelengths, (d) dependences of the same characteristic on the wavelength in the range of 400 to 700 nm for specified incidence angles.

It is also necessary to take into account that when the output signals of the optical system are formed, there is a cross-influence of adjacent wavelengths for each of the system units, since the spectral functions of the source, photodetectors and reflective film are quite broadband. Therefore, the transfer functions of the optical units should be integrated over the wavelength in the entire relevant spectral range [26].

Hence, the resulting transfer function will consist of the product of the spectral function of the white light source $E(\lambda)$, the spectral function of the webcam photodetectors $Q_k(\lambda)$ (separately for each k-th color component), and the spectrum of the light reflectance coefficient $R(\lambda, \theta)$ under the conditions of SPR excitation. The angle θ acts as a fixed parameter from the range of actual incidence angles. The values of the output signals for each of the R, G and B components $\rho_k(\theta)$ are determined by the following integral expressions:

$$\rho_k(\theta) = \int E(\lambda) R(\lambda, \theta) Q_k(\lambda) d\lambda, \; k \in \{R, G, B\}, \qquad (1)$$

where all the spectral functions under the integral are normalized in a unit scale, and the integral is calculated over the entire visible spectrum wavelength range ($\Delta\lambda = 400\ldots700$ nm). Note that belonging of the value of $\rho_k(\theta)$ to one of the three color signals $k \in$ R, G, B is embedded in the differences in the spectral functions of the webcam photodetectors $Q_k(\lambda)$. The functional dependence of $\rho_k(\theta)$ on θ is formed by the dependence of the spectrum of reflected light $R(\lambda, \theta)$ on the incidence angle.

Since the values $\rho_k(\theta) = \{R(\theta), G(\theta), B(\theta)\}$ are in the range of 0...1, the next stage of the calculation was transformation of these values from relative units into a graphic format (in fact, this is multiplication by 255, corresponding to a factor of 2^8 shades in a computer color gradation scale). Note that such a representation of the color components depends on presence and illumination of neighboring pixels [27]. However, considering that we are not dealing here with a finely detailed spectral picture, and transitions of the color components occur quite smoothly, it seems possible not

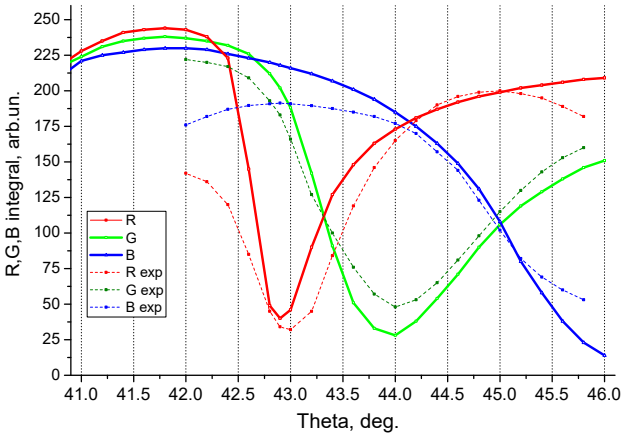

Fig. 3. Calculated values of color components R(θ), G(θ), B(θ) obtained by expression (1) taking into account the real spectral functions of all the optical elements (solid curves). For comparison, experimental R, G, B dependences are also shown (dashed curves).

to take into account the influence of the neighboring pixels. The resulting values of the color components R, G, B in the scale of the angles of light incidence obtained by the method described above are shown in Fig. 3. For comparison, the same R, G, B curves extracted from the experimental reflection spectrum (see Fig. 1b), obtained under the same conditions as the calculated dependences, are shown by dotted lines in the same figure.

The final stage of the calculations is transformation of the angular dependence of the above color components R, G, B into a corresponding spectral picture of the reflected light. In the computer representation of colors, such a transformation of three values R, G, B into color is carried out according to the formula RGB:Color = R + 256·G + 65536·B.

Fig. 4 shows the resulting calculated spectral pattern of the reflected light on an angular scale. The actual reflection spectrum obtained from the experiment is shown next to it for comparison. The calculated spectrum (Fig. 4a) is shown as a set of spectral bands, where the sections adjacent by the incidence angle have a shape of rectangles with a minimum step of 12 angular minutes (0.2 degree). Each such section is colored according to the triple of R, G, B values obtained from the curves of Fig. 3 and a perpendicular drawn through the center of the rectangle. The experimental reflection spectrum (Fig. 4b) is shown on the same angular scale for ease of comparison.

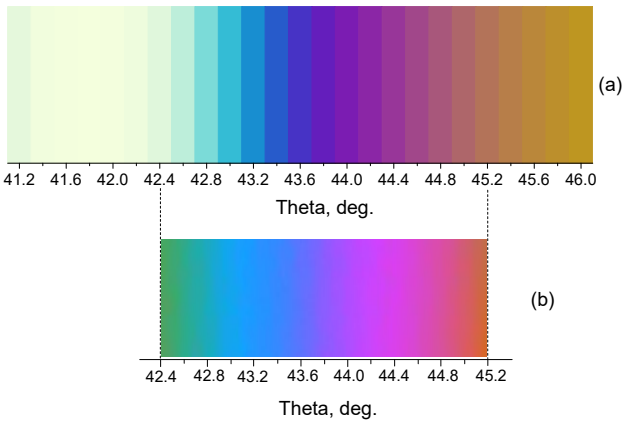

Fig. 4. (a) Model integral reflection spectrum in an angular scale from 41 to 46 degrees calculated with an angular step of 0.2 degree and (b) real experimental reflection spectrum obtained from the webcam output.

Comparison of the calculated and experimental curves R(θ), G(θ), B(θ) shows that they are quite close (see Fig. 3), and the spectral patterns visible by an eye (Fig. 4) qualitatively coincide. Only some differences are noticeable on the left edge of the angular scale. These differences can be explained by instrumental distortions of the webcam signals at the edges of the operating range. Nevertheless, the very close similarity of the main part of the calculated and experimental spectra in Figs. 3 and 4 leaves no doubt about correctness of the proposed model approach as a whole. Note that it is difficult to expect complete coincidence of the spectra due to a number of reasons: a non-point light source, a finite slit width, uneven beam divergence, inhomogeneities of the metal film, experimental error in measuring the spectra of photodetectors, *etc*.

3. Influence of external environment on the reflectance spectrum during SPR

The condition for excitation of plasmon-polariton resonance is the equality of the wave vectors of the surface plasmon (SP) at the metal-medium interface, k_{spr}, and the longitudinal component of the *p*-polarized light wave at the metal-glass interface, k_x:

$$k_{spr} = (\omega/c)\left[\varepsilon_m(\lambda)\varepsilon_d/\varepsilon_m(\lambda)+\varepsilon_d\right]^{1/2}, \quad k_x = (\omega/c)N_g \sin\theta \quad . \tag{2}$$

From here, the well-known expression for the angle of minimum SPR follows:

$$N_g \sin\theta = \sqrt{\frac{\varepsilon_m(\lambda)\varepsilon_d}{\varepsilon_m(\lambda)+\varepsilon_d}} \quad . \tag{3}$$

Here, N_g is the refractive index of glass, $\varepsilon_m(\lambda)$ is the real part of the permittivity of a metal, and ε_d is the dielectric constant of the external environment, $\varepsilon_d = n^2$, where n is the refractive index of the medium (gas).

From the expression (2), we find the change in the wave vector of surface plasmon k_{spr} for small variations in the permittivity of the external environment. With an increase in ε_d by a small value $\Delta\varepsilon_d$, the wave vector of the SP will increase by the value

$$\Delta k_{spr} = \frac{dk_{spr}}{d\varepsilon_d}\Delta\varepsilon_d \, ,$$

where

$$\frac{dk_{spr}}{d\varepsilon_d} = \frac{1}{2\sqrt{\varepsilon_d}}\left(\frac{\varepsilon_m}{\varepsilon_m+\varepsilon_d}\right)^{3/2} \quad . \tag{4}$$

Under the SPR conditions (*i.e.* at $\varepsilon_d < -\varepsilon_m$), the derivative $dk_{spr}/d\varepsilon_d$ is a positive value. Therefore, the plasmon wave vector increases at an increase in ε_d. According to (3), this leads to an increase in sinθ and the angle itself θ_{min}, *i.e.*, to a shift of the curves $\rho_k(\theta) = \{R(\theta), G(\theta), B(\theta)\}$ to the right on the angle scale. This is demonstrated in Fig. 5, which shows angular dependences of the values of R(θ), G(θ), B(θ) calculated using Eq. (1) on the computer scale of color components at the values of the refractive index of the medium increasing from 1.000 to 1.003 with a step of 0.001.

As an important feature of the curves shown in Fig. 5, we note two regions of the highest "color contrast speed" when scanning along the incidence angle. These are the regions at 43.4 deg. and 44.9 deg. marked with vertical arrows. At such angles, the ascending and descending branches of two components intersect, namely R and G at 43.4 deg., and G and B at 44.9 deg. The indicated features are important for optimizing the responses recording mode of a chromatic SPR sensor. Indeed, the value of ε_d increases upon contact with an analyte gas, and the reflection spectrum curve should shift toward larger incidence angles. Since the changes in the R-G and G-B component pairs are in different directions, the difference between these components will be greater, the greater the difference in the refractive index of the analyzed sample from the control one. This fact can be successfully used to increase the response signal by recording the difference in the values of the component pairs.

The curves shown in Fig. 5 allow us to estimate the real instrumental sensitivity of the chromatic SPR sensor to small changes in the refraction index of the external environment. As can be seen from this figure, all the curves shift almost parallel. The angular value of the shift is approximately $\Delta\theta = 0.07\ldots0.08$ degrees at the change in the refractive index $\Delta n = 0.001$. Therefore, according to the criterion of the angle shift of the SPR curve minimum, the sensitivity was 70 deg/RIU ($\Delta\theta/\Delta n$) for the *R* component, 75 deg/RIU for the G component and 85 deg/RIU for the B component, respectively.

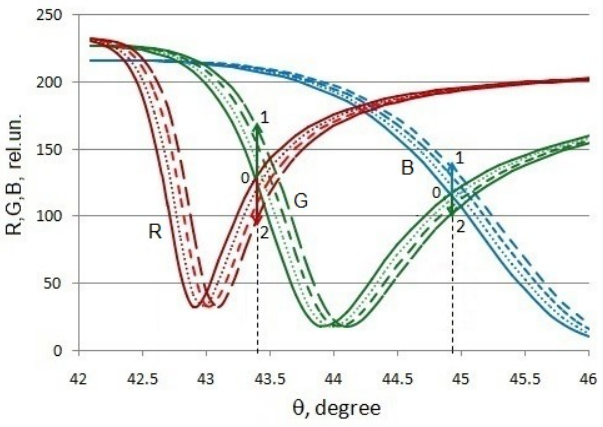

Fig. 5. Calculated values of R(θ), G(θ), B(θ), obtained from expression (1) at the values of the refractive index of the medium of 1.000 (solid line), 1.001 (dashed line), 1.002 (short dashed line) and 1.003 (long dashed line).

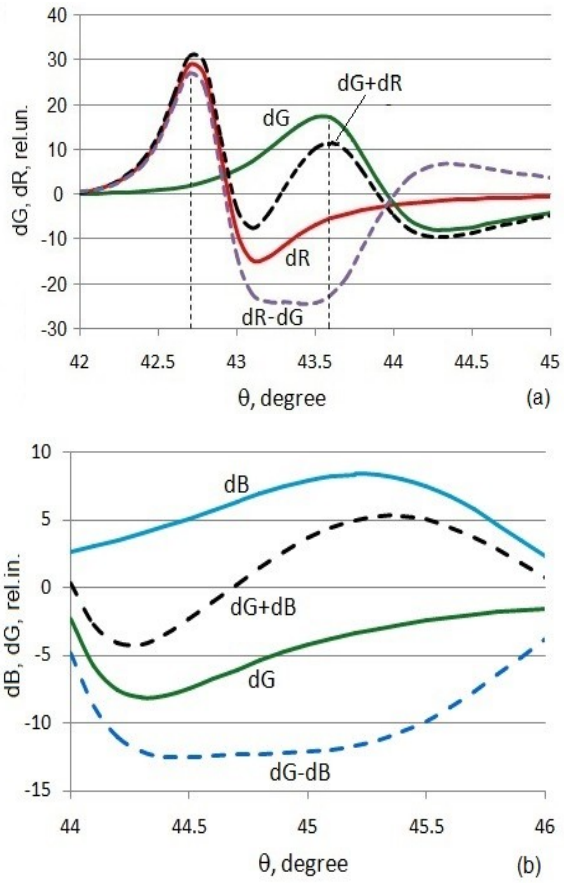

Fig. 6. Responses of the dR, dG components and their combinations for incidence angles of 42° to 45° (a) and the dG, dB components and their combinations for angles of 44° to 46° (b) at an increase in the refractive index of the medium by 0.001. The dotted line indicates the peak values of the dR and dG responses at angles of 42.7° and 43.6°, respectively.

From the point of view of one of the objectives of this work, namely, search for approaches to creating new design options for a polychromatic SPR sensor based on registration of the color of the reflected beam, we will consider in more detail the above-mentioned trend of the opposite change in the pairs of the components R-G and G-B. Thus, taking into account the data in Fig. 5, the following Fig. 6 demonstrates angular dependences of the indicated difference combinations of color components at increasing the refractive index of the external environment by 0.001.

As follows from Fig. 6a, the dG and dR signals noticeably change their magnitude and even sign when the incidence angle changes within the interval 42°…45°. Note that the amplitudes of the dR and dG signals at fixed angles of 42.7° and 43.6°, at which these signals have peak values, can be successfully used as response signals for a polychromatic sensor in an optical scheme with a slightly diverging white light beam. To achieve maximum sensitivity, the amplitudes of the dR and dG signals at the specified angles can be summed up, which will increase the response to a change of $\Delta n = 0.001$ by almost twice.

However, it seems more promising to use the difference combination of the responses dR-dG, which demonstrates a horizontal section over more than half a degree between the angles 43 and 43.6 deg. and at the same time a sufficiently high response level. This opens up a possibility of averaging the signal over a sufficiently extended section of the image and increasing the reliability of recording Δn by changing the color of the reflected beam. (Note that the total combination dG + dR turns out to be useless in this case.)

A similar picture is observed for the pair dG and dB (Fig. 6b). Here, the difference combination dG-dB also demonstrates a horizontal section between the angles 44.5 and 45.5 deg., which even exceeds the length of that in Fig. 6a. However, the response values in this case are clearly smaller, and, hence, the sensitivity of registration of Δn will be noticeably lower.

It should be concluded from the presented analysis that presence of horizontal sections on angular dependences of the difference of the color components dR-dG and dG-dB allows us to switch to using the collimated incident light beams instead of weakly diverging ones. In this case, the incidence angle of the collimated beam can be chosen constant with any value from the above mentioned half-degree ranges of angles for the dR-dG and dG-dB responses.

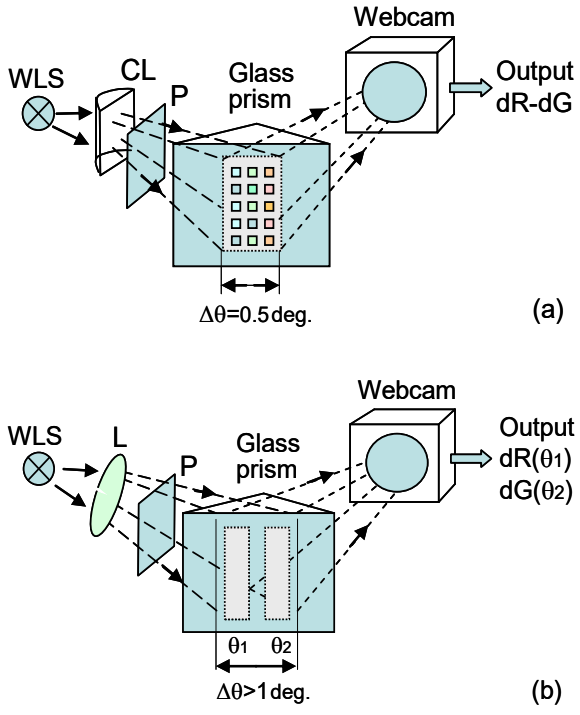

Fig. 7. Optical schemes for implementing polychromatic SPR with optimal modes for registering optical signals: (a) operation with a relatively parallel beam (divergence up to 0.5 deg. in the angular range of 43° to 43.5°) and registration of the difference signal dR-dG, (b) use of a diverging beam and registration of signals of the color components dR and dG at two different angles of light incidence of 42.7 and 43.6 deg., respectively. WLS – white light source, CL – collimating lens, P – polarizer.

To summarize this consideration, the following options for operation of a polychromatic SPR sensor may be suggested:

1) To operate on the plateau in the angular range of 43° to 43.5° for a relatively *parallel* beam (with the maximum divergence of no more than 0.5 degrees) and registration of only the difference signal dR-dG. Note that due to the half-degree divergence of the beam, it is convenient in this case to form a 2D matrix of miniature sensors on the silver surface located in the region of plateau, both in the longitudinal and transverse directions relative to the angular sweep line (Fig. 7a).

2) To use a *diverging* beam (with the divergence of more than 1 degree), while recording the signals of two color components at two fixed angles, namely the dR signal at $\theta_1 = 42.7°$, and the dG signal at $\theta_2 = 43.6°$. Obviously, it is possible to form arrays of 1D sensor matrices located perpendicular to the angular sweep line at the two specified angles in this case (Fig. 7b).

3) To work with a parallel beam at the angles of 44.5° to 45.5° (in the plateau region with registration of the difference signal dG-dB), which should be structurally simpler, but the response sensitivity in this case is expected to be approximately 2 times less.

Therefore, the advantage of the described approach is that it uses one white light source and three color responses. At the same time, we take advantage of different wavelengths without using complex optical schemes. This provides the possibility of significant miniaturization of the sensor optical system and an increase in its productivity with simultaneous analysis of multiple sensor cells. An important advantage of the proposed approach is the ability to programmatically select the registration angle, which opens a way to full automation of measurements.

4. Options for implementing polychromatic SPR sensors without using a webcam as a response recorder

Comparison of the obtained integral angular functions of the color components R, G, B (see Fig. 3) with the initial angular dependences of the reflection coefficient of the silver film presented in Fig. 2c shows that there are no qualitative changes in the curves after taking into account the spectra of the source and photodetectors, with the exception of a quantitative change in the ratio of angles, depth and width of the SPR minima. This suggests that the main contribution to the integral color functions is made by the spectral dependence of the reflection coefficient $R(\lambda,\theta)$, while the spectral dependences of the light source $E(\lambda)$ and the webcam photodetectors $Q_k(\lambda)$ influence only the details of the resulting reflection spectrum but do not change its overall view. This makes it possible to implement a number of simplified versions of optical circuits of a polychromatic SPR sensor by combining different types of light sources and receivers, in particular, without using a video camera as a response signal recorder. Similar versions of circuits with registration of two color components R and G of the reflected light are shown in Fig. 8.

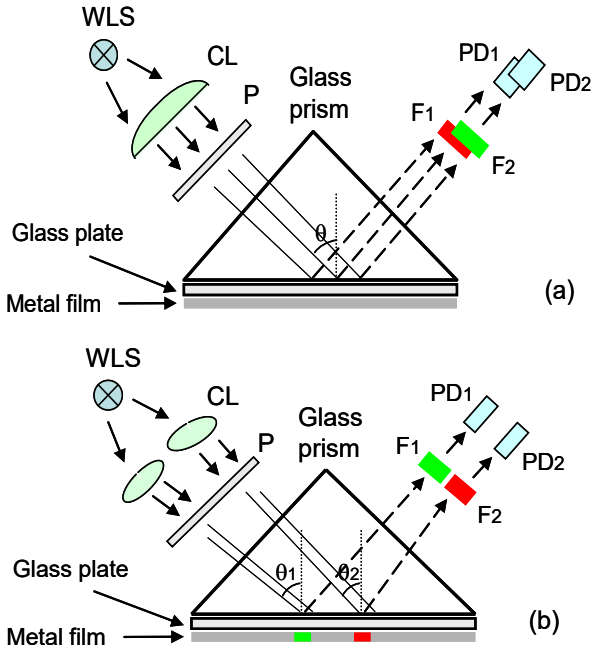

Fig. 8. Optical schemes for implementation of spectral SPR using photodiodes for recording the response: (a) scheme with a relatively parallel beam with a maximum divergence of up to 0.5 deg., (b) scheme with fixed angles of light incidence θ_1 and θ_2. F_1 and F_2 – bandpass color filters, PD_1 and PD_2 – discrete photodiodes.

The optical scheme in Fig. 8a implements the above-described idea of using a plateau for the difference signal dR-dG in the angular range of 43° to 43.5° (see Fig. 7a) and operation with a relatively parallel light beam on the slopes of the SPR curves R(θ) and G(θ). The collimator is adjusted to provide only a small beam divergence within no more than 0.5 degrees in the plateau region. To simplify and reduce the cost of the design, conventional discrete photodiodes (PD) are used instead of a webcam. These photodiodes are located along a fixed angle line one above another. However, since the photodiodes must register only individual R and G components in a fairly narrow wavelength band, red and green bandpass color filters, respectively, must be placed on the way of the reflected beam. Each PD registers a change in the intensity of only one of the specified color components, and a differential response signal is formed at the output.

Fig. 8b also shows a photodiode version of the optical scheme, but with parallel beams with two fixed angles of incidence θ_1 and θ_2, which are formed by two separate collimators. Here, the operating mode is implemented on the slopes of the R(θ) and G(θ) curves with bandpass filters to eliminate cross-influence of the color components. Both photodiodes are located at some distance from each other and register two separate signals $dR(\theta_1)$ and $dG(\theta_2)$ at the specified angles, where they are maximal.

Note that replacing webcam photodetectors with photodiodes will, of course, lead to a certain change in the spectral function $Q_k(\lambda)$, which in this case will be determined by the transmission spectrum of the bandpass filters. This will entail certain differences in the calculated values of the resulting transfer function (1), and, accordingly, some changes of the angular values for the plateau of the difference signal dR-dG, as well as the values of the angles θ_1, θ_2 for recording the responses $dR(\theta_1)$ and $dG(\theta_2)$. Note also that, within the framework of further simplification of the element base, the white light source can, in principle, be replaced by a set of separate monochromatic R, G, B LEDs. In this case, it will also be necessary to take into account the influence of the variation of the spectral function of the light source $E(\lambda)$ on the resulting output signal.

Therefore, in the above-described implementations of polychromatic SPR sensors, use of only two wavelengths makes it possible to record changes in the refractive index of a gaseous medium without using a video camera.

5. Conclusions

By modeling the resulting integral reflection spectra, a method for assessing the instrumental sensitivity of a chromatic SPR sensor in the Kretschmann geometry to changes in the parameters of the external environment has been developed based on account of the transfer characteristics of all components of the optical system (radiation source, R, G, B signal photodetectors and plasmon-generating structure) in the visible light wavelength range.

Based on the proposed method, the values of the instrumental sensitivity to small changes in the refraction index of the external environment were obtained according to the criterion of the angular shift of the R, G, B curves of the reflection spectrum. This shift was 70 deg/RIU for the R component, 75 deg/RIU for the G component and 85 deg/RIU for the B component.

Comparison of the obtained model reflection spectrum with the real experimental spectrum showed their close similarity. It follows from this similarity that the proposed model approach is fair and, hence, the obtained estimates of the sensitivity of the chromatic SPR sensor are adequate.

Approaches to creating new versions of polychromatic SPR sensors for gas analysis based on registration of the color of the reflected beam are proposed. It is shown that use of difference signals of color components in the optical scheme of the SPR sensor with fixed light incidence angles allows for higher sensitivity to the changes in the refractive index of the medium or adsorption of volatile molecules on a silver film, including not using a video camera as a response recorder.

References

1. Homola J., Yee S. Gauglitz G. Surface plasmon resonance sensors: Review. *Sens. Actuators B: Chem*. 1999. **54**. P. 3–15. http://doi.org/10.1016/S0925-4005(98)00321-9.

2. *Handbook of Surface Plasmon Resonance*, 2nd Edition, Eds. R.B.M. Schasfoort. The Royal Society of Chemistry. 2017. https://doi.org/10.1039/9781788010283-FP010.
3. Huang Y.H., Ho H.P., Wu S.Y., Kong S.K. Detecting phase shifts in surface plasmon resonance: A review. *Adv. Opt. Technol.* 2012. **2012**. Article ID 471957(12 p.). https://doi.org/10.1155/2012/471957.
4. Kukla O.L., Shirshov Yu.M., Biletskiy A.I., Fedchenko O.N. Spectral SPR effect in thin films of high-conductive metals and features of implementation of SPR-biosensors in chromatic mode. *SPQEO.* 2024. **27**. P. 478–488. https://doi.org/10.15407/spqeo27.04.478.
5. Pollet J., Delport F., Janssen K.P.F. *et al.* Fast and accurate peanut allergen detection with nanobead enhanced optical fiber SPR biosensor. *Talanta*. 2011. **83**, Issue 5. P. 1436–1441. https://doi.org/10.1016/j.talanta.2010.11.032.
6. Loo J.F.-C., Lau P.-M., Kong S.-K., Ho H.-P. An assay using localized surface plasmon resonance and gold nanorods functionalized with aptamers to sense the cytochrome-c released from apoptotic cancer cells for anti-cancer drug effect determination. *Micromachines.* 2017. **8**, No 11. P. 338. https://doi.org/10.3390/mi8110338.
7. Hu D.J.J., Ho H.P. Recent advances in plasmonic photonic crystal fibers: Design, fabrication and applications. *Adv. Opt. Photonics.* 2017. **9**, No 2. P. 257–314. https://doi.org/10.1364/AOP.9.000257.
8. Sotnikov D.V., Zherdev A.V., Dzantiev B.B. Surface plasmon resonance based miniaturized biosensors for medical applications, In book: *Nanobiosensors for Personalized and Onsite Biomedical Diagnosis*, 2016. P. 499–520. https://doi.org/10.1049/PBHE001E_ch24.
9. Ho A.H.-P., Kim D., Somekh M.G. (Eds.) *Handbook of Photonics for Biomedical Engineering*, Springer Science+Business Media, Dordrecht, 2017. https://doi.org/10.1007/978-94-007-5052-4.
10. Fasoli J.B., Corn R.M. Surface enzyme chemistries for ultrasensitive microarray biosensing with SPR imaging. *Langmuir*. 2015. **31**, No 35. P. 9527–9236. https://doi.org/10.1021/la504797z.
11. Lebourgeois V., Bégué A., Labbé S. *et al.* Can commercial digital cameras be used as multispectral sensors? A crop monitoring test. *Sensors.* 2008. **8**, No 11. P. 7300–7322. https://doi.org/10.3390/s8117300.
12. Chen C., Hui D., Qi S., Han C. Smartphone-based spectrometer with high spectral accuracy for mHealth application. *Sens. Actuators A*. 2018. **274**. P. 94–100. https://doi.org/10.1016/j.sna.2018.03.008.
13. Long K.D., Woodburn E.V., Le H.M. *et al.* Multimode smartphone biosensing: the transmission, reflection, and intensity spectral (TRI)-analyzer. *Lab Chip*. 2017. **17**. P. 3246–3257. https://doi.org/10.1039/C7LC00633K.
14. Huang X., Xu D., Chen J. *et al.* Smartphone-based analytical biosensors. *Analyst*. 2018. **143**. P. 5339–5351. https://doi.org/10.1039/C8AN01269E.
15. McGonigle A.J.S., Wilkes T.C., Pering T.D. *et al.* Smartphone spectrometers. *Sensors*. 2018. **18**, No 1. P. 223. https://doi.org/10.3390/s18010223.
16. Crocombe R.A. Portable spectroscopy. *Appl. Spectrosc*. 2018. **72**, No 12. P. 1701–1751. https://doi.org/10.1177/0003702818809719.
17. Zhang C., Cheng G., Edwards P. *et al.* G-Fresnel smartphone spectrometer. *Lab Chip*. 2016. **16**. P. 246–250. https://doi.org/10.1039/C5LC01226K.
18. Grossi M. A sensor-centric survey on the development of smartphone measurement and sensing systems. *Measurement*. 2019. **135**. P. 572–592. https://doi.org/10.1016/j.measurement.2018.12.014.
19. Wang L.-J., Chang Y.-C., Sun R., Li L. A multichannel smartphone optical biosensor for high-throughput point-of-care diagnostics. *Biosensors and Bioelectronics*. 2017. **87**. P. 686–692. https://doi.org/10.1016/j.bios.2016.09.021.
20. Melman Y., Wells P.K., Katz E., Smutok O. A universal nanostructured bioanalytical platform for NAD^+-dependent enzymes based on the fluorescent output reading with a smartphone. *Talanta*. 2022. **243**. P. 123325. https://doi.org/10.1016/j.talanta.2022.123325.
21. Wong C.L., Chen G.C.K., Ng B.K. *et al.* Multiplex spectral surface plasmon resonance imaging (SPRI) sensor based on the polarization control scheme. *Opt. Express*. 2011. **19**, No 20. P. 18965–18978. https://doi.org/10.1364/OE.19.018965.
22. Lin T.-Z., Chen C.-H., Lei Y.-P., Huang C.-S. Gradient guided-mode resonance biosensor with smartphone readout. *Biosensors*. 2023. **13**. P. 1006. https://doi.org/10.3390/bios13121006.
23. Zybin A., Grunwald C., Mirsky V.M. *et al.* Double-wavelength technique for surface plasmon resonance measurements: Basic concept and applications for single sensors and two-dimensional sensor arrays. *Anal. Chem.* 2005. **77**. P. 2393–2399. https://doi.org/10.1021/ac048156v.
24. Riabchenko O.V., Kukla O.L., Fedchenko O.N. *et al.* SPR chromatic sensor with colorimetric registration for detection of gas molecules. *SPQEO.* 2023. **26**. P. 343–351. https://doi.org/10.15407/spqeo26.03.343.
25. Azzam R.M.A., Bashara N.M. *Ellipsometry and Polarized Light.* North-Holland Publishing Company, 1977.
26. Finlayson G.D. Colour and illumination in computer vision. *Interface Focus*. 2018. **8**, No 4. P. 20180008. http://doi.org/10.1098/rsfs.2018.0008.
27. Burggraaff O., Schmidt N., Zamorano J. *et al.* Standardized spectral and radiometric calibration of consumer cameras. *Opt. Express*. 2019. **27**, No 14. P. 19075. https://doi.org/10.1364/OE.27.019075.

Authors and CV

O.L. Kukla, Doctor of Sciences in Physics of Devices, Elements and Systems, Head of the Department of Chemobiosensorics at the V. Lashkaryov Institute of Semiconductor Physics. The area of his scientific activity includes development and design of chemical and biological sensors, sensor arrays for biotechnology, medicine and ecology, and study of molecular adsorption effects in polymer, biopolymer and composite thin layers.
https://orcid.org/0000-0003-0261-982X

Yu.M. Shirshov, Doctor of Sciences in Physics and Mathematics (1991), Professor – scientific consultant at the V. Lashkaryov Institute of Semiconductor Physics. The area of his scientific interests includes molecular phenomena on semiconductor and insulator surfaces, optoelectronic and microelectronic chemical sensors and biosensors.
E-mail: y_shirshov@hotmail.com

O.N. Fedchenko graduated from the Lviv Polytechnical Institute in 1964 by the specialty "Semiconductor Devices". Since 2010 he is a Researcher at the V. Lashkaryov Institute of Semiconductor Physics. His scientific interests include color RGB-spectroscopy of thin-film chemical gas sensors and development of optoelectronic colorimetric analyzers.
E-mail: fedchenkoaleksandr50@gmail.com

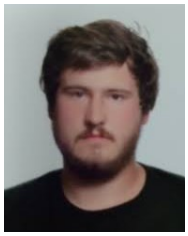

A.I. Biletskiy graduated from the Taras Shevchenko National University of Kyiv with the MSc degree in Applied Physics. PhD Student (2023) and Engineer (2024) at the V. Lashkaryov Institute of Semiconductor Physics. His professional activities include development of an optical measuring setup based on surface plasmon resonance and spectroscopy study of radiation from plasmon-photon scattering in thin films of high conducting materials.
E-mail: belanton11@gmail.com,
https://orcid.org/ 0009-0007-2074-3839

O.S. Kondratenko, PhD in Physics and Mathematics, Researcher at the Department of Polaritonic Optoelectronics and Technology of Nanostructures, V. Lashkaryov Institute of Semiconductor Physics. The area of her scientific interests includes optoelectronics, plasmonics, optics, nanophotonics, and thin films. https://orcid.org/0000-0003-1948-4431, e-mail: ol.s.kondratenko@gmail.com

Authors' contributions

Kukla O.L.: project administration, methodology, visualization, formal analysis, writing – original draft, writing – review & editing.
Shirshov Yu.M.: conceptualization, formal analysis, writing – original draft.
Biletskiy A.I.: methodology, formal analysis, software, data curation, visualization.
Fedchenko O.N.: investigation, validation, resources.
Kondratenko O.S.: data curation, resources.

Оптимізація хроматичного ППР сенсора газового середовища на основі реєстрації кольору відбитого променя: Моделювання та експеримент

О.Л. Кукла, Ю.М. Ширшов, А.І. Білецький, О.М. Федченко, О.С. Кондратенко

Анотація. Проведено розрахунок оптичних характеристик хроматичного сенсора для детектування газових середовищ на основі ефекту плазмон-поляритонного резонансу (ППР) при реєстрації відгуків по колірному спектру відбитого променя при врахуванні спектральних характеристик всіх складових оптичної системи (джерела випромінювання, фотоприймачів і багатошарової відбиваючої структури) в діапазоні довжин хвиль видимого світла. На основі цього розрахунку запропоновано методику оцінки апаратної чутливості ППР сенсора до зміни параметрів зовнішнього середовища (показника заломлення або діелектричної проникності). Для моделювання та експерименту як чутливий елемент використовувалась тонка срібна плівка на базовій грані призми в геометрії Кречмана, що дозволило забезпечити повноцінний ефект ППР у всьому видимому спектральному діапазоні 400–700 нм. Реалізовано колориметричну реєстрацію спектрів відбиття за допомогою кольорової веб-камери з вихідними сигналами R,G,B в ролі оптичного відгуку.

Ключові слова: спектральний ППР, хроматичний режим, плівка срібла, оптичний газовий сенсор, колориметрична реєстрація, спектр відбитого променя, R,G,B компоненти, область видимого світла.